Synthesis of Aminosilane Chemical Vapor Deposition Precursors and Polycarbosilazanes through Manganese Catalyzed Si-N Dehydrocoupling

Thao T. Nguyen,[†] Tufan K. Mukhopadhyay,[†] Samantha N. MacMillan,[‡] Michael T. Janicke,[§] Ryan J. Trovitch*,[†]

[†]*School of Molecular Sciences and Biodesign Center for Sustainable Macromolecular Materials and Manufacturing, Arizona State University, Tempe, Arizona 85287, United States*

[‡]*Department of Chemistry and Chemical Biology, Baker Laboratory, Cornell University, Ithaca, New York 14853, United States*

[§]*Chemistry Division, Los Alamos National Laboratory, Los Alamos, New Mexico 87545, United States*

KEYWORDS

Waste Prevention, Atom Economy, Catalysis, Earth-Abundant Metal, Amines, Silane

ABSTRACT

Compounds that feature Si–N bonds are of widespread importance to the electronics and coatings industries. Aminosilanes and polysilazanes are currently prepared by adding amines to halosilanes, an inefficient methodology that generates stoichiometric quantities of ammonium salt waste. Herein, we describe the syntheses of aminosilane chemical vapor deposition precursors, polycarbosilazanes, and perhydropolysilazane through the ambient temperature dehydrocoupling of amines to silane (SiH_4). Specifically, the β-diketiminate manganese hydride dimer $[(^{2,6\text{-}i\text{Pr2Ph}}BDI)Mn(\mu\text{-}H)]_2$ has been used to catalyze the formation of commercial aminosilane monomers from secondary and primary amines, highly cross-linked polycarbosilazane powders from diamines and triamines, and perhydropolysilazane from ammonia. The mechanism of dehydrocoupling was explored and the addition of isopropylamine to $[(^{2,6\text{-}i\text{Pr2Ph}}BDI)Mn(\mu\text{-}H)]_2$ resulted in σ-bond metathesis to eliminate H_2 and generate $[(^{2,6\text{-}i\text{Pr2Ph}}BDI)Mn(\mu\text{-}NHiPr)]_2$. In the presence of SiH_4, H–Si addition across newly formed Mn–N bonds regenerates the precatalyst, offering a straightforward catalytic cycle for halogen-free Si–N bond formation.

INTRODUCTION

Silicon nitride and silicon carbonitride coatings are widely used in industry because they offer a unique combination of chemical stability and superior mechanical properties.[1,2] These films exhibit outstanding electrical resistivity (10^{12}-10^{17} Ω·cm) and high dielectric strength (10^{6}-10^{7} V/cm), rendering them ideal for protecting microelectronics, photonic devices, and solar cells.[3] Silicon nitride and silicon carbonitride thin films can be prepared using atomic layer deposition (ALD), chemical vapor deposition (CVD), and plasma-enhanced chemical vapor deposition (PECVD). Silicon nitride films obtained by ALD, CVD, and PECVD are essential for the production of integrated circuitry, microprocessors, and memory devices.[4-7]

The most common silicon sources for CVD and ALD include perhydridosilanes, hydridohalosilanes, halosilanes, and aminosilanes. High quality silicon nitride films can be obtained directly from SiH_4 and NH_3 above 300 °C,[3] or at lower temperatures (100–110 °C) by microwave PECVD.[8] Despite their corrosive nature, hydridohalosilanes and halosilanes including SiH_2Cl_2,[9] SiH_2I_2,[10] Si_2Cl_6[11] are often employed under forcing conditions (**Fig. 1a**). Aminosilanes, which can be handled as liquids near ambient conditions, are versatile precursors that can afford either silicon nitride or silicon carbonitride films.[12,13] Unfortunately, aminosilanes are themselves prepared by reacting corrosive iodosilanes[14] or chlorosilanes[15] with the respective amine (**Fig. 1b**). Alternatively, silicon nitride films can be synthesized by pyrolyzing perhydropolysilazane (PHPS, **Fig. 1c**). Once applied to a surface, this polymer can be cross-linked at 200–500 °C to form an amorphous ceramic layer that crystallizes at higher temperatures (700–1260 °C).[16] When hydrolysis is allowed to occur during PHPS curing, silicon oxynitride and silicon dioxide layers are generated,[17,18] which are particularly useful gate dielectrics for thin film transistors.[19] Industrially, PHPS solutions are prepared by reacting chlorosilanes with excess NH_3 in polar solvents such as Et_2O, THF, or DCM.[20,21] Although this approach is straightforward, it is inherently atom-inefficient since one equivalent of NH_4Cl waste is generated for each Si–N bond that is formed, leading to additional purification measures that compromise sustainability and add to process cost.

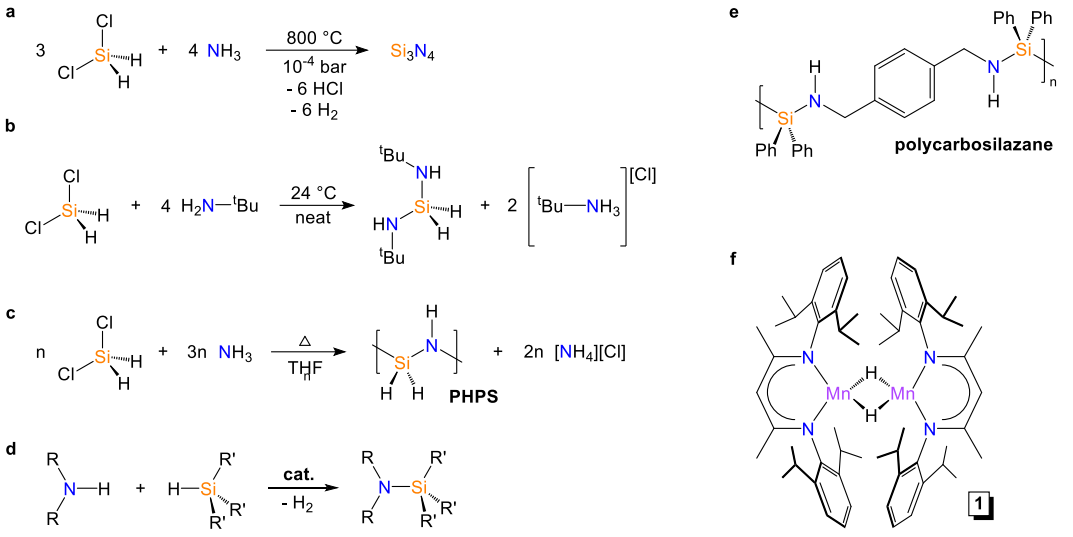

Fig. 1. Methods of preparing Si–N bonds, a representative polycarbosilazane, and the catalyst used in this contribution. **a.** Preparation of silicon nitride from SiH_2Cl_2 and NH_3. **b.** Atom-inefficient synthesis of aminosilane CVD precursor $H_2Si(NHtBu)_2$. **c.** Use of SiH_2Cl_2 to prepare PHPS. **d.** Generation of Si–N bonds via dehydrocoupling. **e.** Polycarbosilazane prepared by Carpentier and Sarazin. **f**. Previously described Mn catalyst **1**.

The dehydrogenative coupling of amines and silanes has long been considered a promising approach to Si–N bond formation that avoids halosilanes (**Fig. 1d**).[22,23] Over the last decade, catalysts featuring elements that span the periodic table including alkaline-earth metals,[24-27] lanthanides,[28] Zn,[29] Pt,[30] and Al[31] have been reported to mediate this transformation. While these studies have used organosilanes to prepare aminosilane monomers, researchers have also demonstrated the preparation of oligocarbosilazanes or polycarbosilazanes using substrates that feature more than one amine functionality. In 2016, Carpentier and Sarazin found that $Ba[CH(SiMe_3)_2]_2(THF)_3$ is an effective catalyst for the dehydrogenative coupling of diphenylsilane and *p*-xylylenediamine to prepare polycarbosilazanes (**Fig. 1e**).[32] This catalyst was shown to generate oligocarbosilazanes in subsequent work.[33] In 2019, the Manners and Hill groups expanded this reactivity to the preparation of ferrocene-containing polycarbosilazanes that yielded magnetic ceramic materials upon pyrolysis.[34] Recently, Webster and co-workers prepared an oligocarbosilazane from 1,4-benzenedimethanamine and phenylsilane using the β-diketiminate iron catalyst, ($^{2,6\text{-}i\text{Pr2Ph}}$BDI)Fe($CH_2TMS$).[35] The oligomers and polymers described in these studies are promising surrogates for industrial organic polysilazanes, which afford thermally-robust and corrosion-resistant coatings on metal surfaces.[36]

In 2018, we reported the synthesis, hydrosilylation activity, and silicone curing ability of the β-diketiminate manganese hydride dimer, [($^{2,6\text{-}i\text{Pr2Ph}}$BDI)Mn(μ-H)]$_2$ (**1**, **Fig. 1f**).[37] This catalyst has also been found to mediate the hydroboration of nitriles to generate diborylamines[38] and an electronic structure investigation revealed that **1** easily dissociates into monomers to enable catalysis.[39] In this study, we demonstrate that **1** is active for the dehydrogenative coupling of amines to the widely utilized industrial gas, SiH_4. In the patent literature, the halogen-free preparation of aminosilane CVD precursors is known to proceed upon heating amines with SiH_4 to 125 °C in the presence of Ru/C;[40] however, this remains the only mention of commercial aminosilane CVD precursor synthesis by way of catalytic Si–N dehydrocoupling. With SiH_4 chosen as the silane source, this contribution details the atom-efficient and halogen-free preparation of aminosilane CVD precursors, polycarbosilazanes, and PHPS at ambient temperature. Taken together, the experiments described herein are believed to be the only reported examples of Mn-catalyzed Si–N dehydrocoupling.

RESULTS

Preparation of CVD Precursors. The preparation of industrially-relevant aminosilanes via dehydrocoupling requires the use of SiH_4 and this starting material can afford a variety of products depending on the number of Si–H bonds that react. Therefore, to minimize complexity, our initial trials focused on the dehydrocoupling of secondary amines that cannot undergo oligomerization or polymerization (**Table 1**). Using a calibrated gas bulb and high-vacuum line, dimethylamine gas (**1a**) was added to a J. Young tube containing 2 mol% of **1** (4 mol% of Mn) in a toluene-d_8 solution featuring 0.2 M tetramethylsilane as an internal standard. To this frozen solution, 1 atm of SiH_4 was added and the reaction was allowed to warm to ambient temperature. After 24 h, greater than 99% conversion of **1a** to a mixture of silylamine products was observed by ^{1}H NMR spectroscopy. Integration against the standard revealed a 73% NMR yield of diaminosilane product $H_2Si(NMe_2)_2$ (**A**, ^{29}Si NMR = -21.54 ppm) and triaminosilane product $HSi(NMe_2)_3$ (**B**, ^{29}Si NMR = -25.09 ppm) in a 1:2.5 ratio. At this point, the experiment was safely decommissioned by freezing the solution in liquid N_2, removing H_2 gas from the headspace, and then recollecting or slowly quenching the residual SiH_4. ***Caution: Silane is a pyrophoric gas that must be handled with care by a skilled experimentalist; for detailed***

experimental procedures and additional safety disclosures, please consult the Supporting Information.

Table 1. Synthesis of CVD precursors via **1**-catalyzed dehydrocoupling of amines and SiH_4.

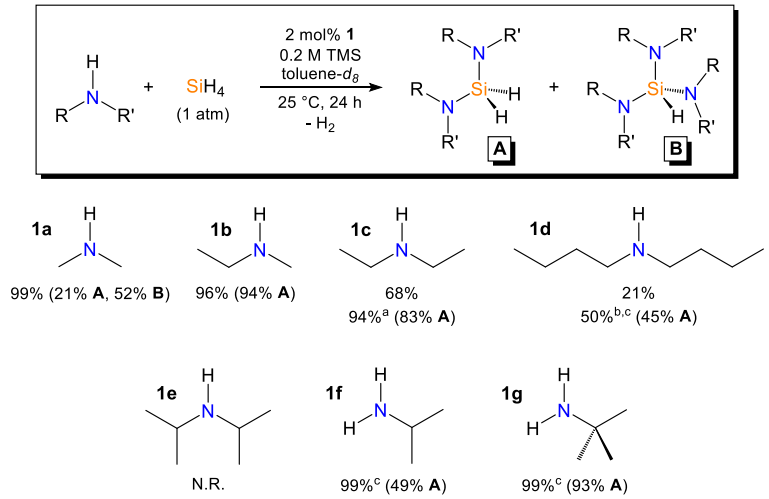

Percent conversion determined by ^{1}H NMR spectroscopy (integration of residual amine vs. silylamine product). NMR yields determined by integration of product against 0.2 M tetramethylsilane standard (shown in parentheses). [a]Trial conducted for 48 h. [b]Trial conducted for 4 days. [c]Trial conducted in a 100 mL bomb instead of J. Young tube.

Using a similar procedure, the steric hinderance of the amine was systematically varied. The **1**-mediated dehydrocoupling of methylethylamine (**1b**) to SiH_4 afforded $H_2Si(NMeEt)_2$ as the sole product in excellent yield. The dehydrocoupling of diethylamine (**1c**) reached 68% conversion after 24 h; however, allowing the reaction to proceed for 48 h allowed for 94% conversion and the selective formation of $H_2Si(NEt_2)_2$. Further lengthening of the alkyl chains to butyl (**1d**) considerably slowed dehydrocoupling, resulting in only 50% conversion to $H_2Si(NBu_2)_2$ after 4 days, even when the reaction was performed in a 100 mL thick-walled glass bomb under a large excess of SiH_4. No reaction was observed at 25 °C in the case of diisopropylamine (**1e**), further demonstrating that steric bulk about the amine inhibits catalysis. After reaching the steric limit of secondary amine dehydrocoupling, we sought to prepare CVD precursors from isopropylamine (**1f**) and *tert*-butylamine (**1g**). When these trials were performed in a J. Young tube, toluene-insoluble polymers were generated, which prevented solution NMR analysis of the product mixture. By repeating these reactions under a large excess of SiH_4,

polymerization was suppressed, affording $H_2Si(NH\textit{i}Pr)_2$ in modest yield and $H_2Si(NH\textit{t}Bu)_2$ in high yield. Importantly, $HSi(NMe_2)_3$, $H_2Si(NEt_2)_2$, and $H_2Si(NH\textit{t}Bu)_2$ are commercial CVD precursors for silicon nitride films that are currently prepared from halosilanes.[41,42]

Preparation of SiH_4-Derived Polycarbosilazanes. Since polymers were observed when dehydrocoupling primary amines under low SiH_4 pressure, we purposely sought to prepare and characterize polycarbosilazane polymers from substrates that feature more than one amine functionality (**Table 2**). In a 100 mL thick-walled glass bomb, 1 atm of SiH_4 was added to a benzene solution of ethylenediamine and 2 mol% of **1**. After 2 h at 25 °C, precipitate was observed and the transformation was allowed to proceed for an additional 22 h to ensure reaction completion. Upon washing with THF to remove residual catalyst, a tan solid identified as polycarbosilazane **2a** was obtained in 60% yield. Product **2a** is highly cross-linked and insoluble in organic solvents, properties that prevent solution-state ^{1}H NMR end-group analysis and estimation of number average molecular weight by ^{1}H DOSY NMR spectroscopy.[32] Subjecting a 1 mg sample of **2a** to THF for 1 week did not allow for observable dissolution; however, analysis of the resulting solution by MALDI-TOF mass spectrometry revealed Gaussian distributions at 469, 695, and 932 g/mol. These peaks are consistent with residual 4-, 6-, and 8-unit oligomers of **2a** that were washed off of the bulk product, which is considered to be an infinite network solid. Solid-state infrared and multinuclear cross-polarization magic angle spinning (CP-MAS) NMR spectroscopy also proved to be informative. The IR spectrum of **2a** was found to feature a strong Si–H stretch at 2131 cm^{-1} and a weak Si–N stretch at 818 cm^{-1}.[43] The ^{15}N CP-MAS NMR spectrum of this product was found to feature a single resonance at 21.64 ppm (**Fig. S19**), while the ^{29}Si NMR spectrum was found to exhibit a minor peak at -36.58 ppm and a major peak at -26.72 ppm for $\textit{Si}N_3H$ and $\textit{Si}N_2H_2$ (**Fig. S20**), respectively.

Table 2. Synthesis of polycarbosilazanes from SiH_4 using **1**.

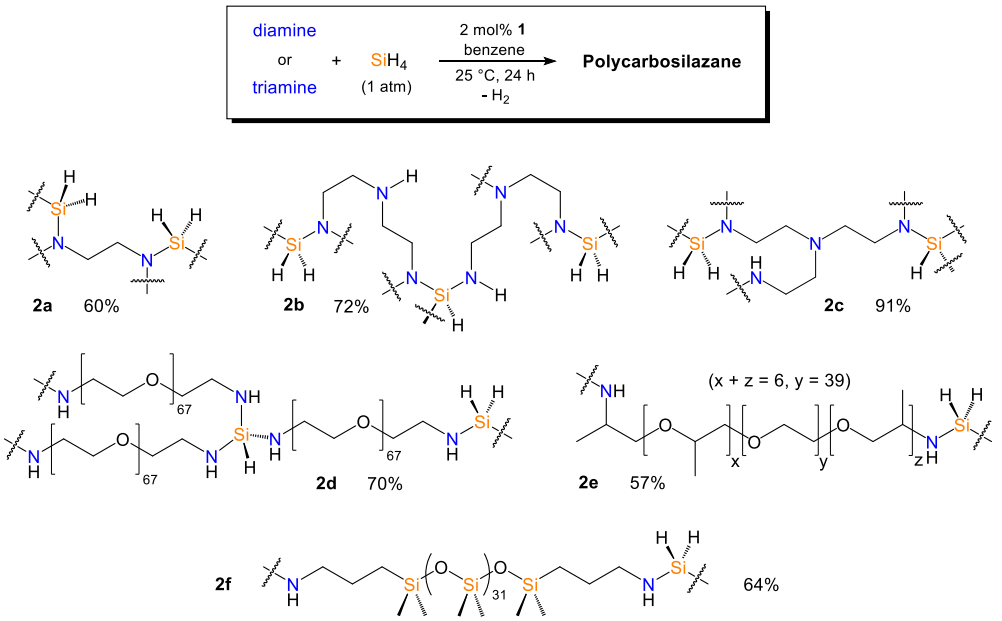

Isolated yields reported relative to diamine or triamine substrate.

Repeating this procedure with diethylenetriamine and tris(2-aminoethyl)amine afforded polycarbosilazanes **2b** and **2c**, respectively. As observed for **2a**, MALDI-TOF mass spectrometry revealed residual low molecular weight oligomers (446, 670, and 900 g/mol) that were washed off of insoluble **2b**. For illustrative purposes, data collected for **2c** is highlighted in **Figure 2**. The infrared spectrum of **2c** (**Fig. 2a**) was found to feature N–H (3293 cm^{-1}), sp^3 C–H (2936-2802 cm^{-1}), Si–H (2110 cm^{-1}), C–N (1103-1048 cm^{-1}), and Si–N (845 cm^{-1}) stretching vibrations (**Fig. 2b**).[43] The ^{15}N CP-MAS NMR spectrum of this product (**Fig. 2c**) revealed a broad, multi-component signal centered at 23.65 ppm due to the presence of silylamine, disilylamine, and tertiary amine environments. Moreover, the ^{29}Si CP-MAS NMR spectrum of **2c** (**Fig. 2d**) revealed a dominant signal at -33.75 ppm that corresponds to SiN_3H environments and a downfield shoulder that suggests the presence of SiN_2H_2 environments. The stability of **2a-2c** towards ambient conditions was also analyzed by infrared spectroscopy. After 1 h of exposure to air featuring 13% humidity, a significant decrease in Si–H and Si–N infrared vibration absorbance was noted for all three compounds (**Table 3**), indicating that these products are easily hydrolyzed.

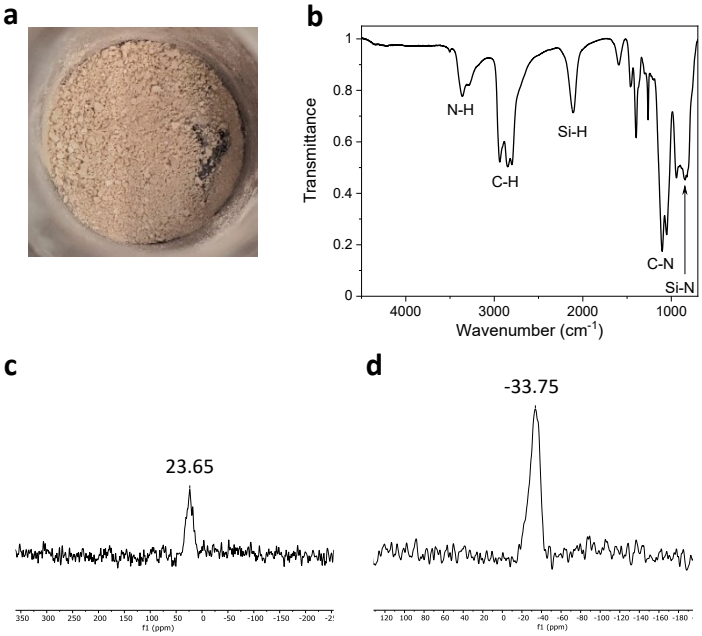

Fig. 2. Characterization of polycarbosilazane **2c**. **a.** Image of solid product. **b.** Solid-state infrared spectrum in KBr. **c.** ^{15}N CP-MAS NMR spectrum. **d.** ^{29}Si CP-MAS NMR spectrum.

Table 3. Percentage decrease in Si–H and Si–N infrared vibration integration after 1 h of exposure to air at 13% humidity.

Polymer	Si–H	Si–N
2a	-49%	-26%
2b	-69%	-34%
2c	-87%	-68%
PHPS	-65%	-85%

The scope of **1**-mediated dehydrocoupling was then extended to amine-terminated polymers. The use of diaminopoly(ethyleneglycol) (M_w = 3000 g/mol) afforded **2d** as a tan solid in 70% yield and elemental analysis suggested the presence of $SiH_2(NHR)_2$ and $SiH(NHR)_3$ moieties. Jeffamine ED-2003, which features methyl substitution at the α- and ω-positions of the polymer chain, was found to yield a waxy white solid possessing $SiH_2(NHR)_2$ linkages (**2e**). Likewise, the dehydrocoupling of bis(3-aminopropyl) terminated poly(dimethylsiloxane) successfully underwent dehydrocoupling with SiH_4 to yield an off-white diaminosilane-bridged polycarbosilazane powder (**2f**). Elemental analysis was particularly helpful for characterizing and assigning the structures of **2d**-**2f**; however, the low N and Si concentration within these products prevented the collection of informative multinuclear CP-MAS NMR data. Accordingly,

the infrared spectra collected for **2d-2f** were found to feature very weak N–H and Si–H stretching vibrations. Products of this type represent attractive alternatives to commercial organic polysilazane anti-corrosion and anti-graffiti coatings prepared through the aminolysis of functionalized chlorosilanes.[44]

Direct Preparation of PHPS. The ability of **1** to generate insoluble polycarbosilazanes when dehydrocoupling primary amines suggested that it might be possible to prepare PHPS in a halogen-free manner from SiH_4 and NH_3. To a 100 mL thick-walled reaction vessel containing a benzene solution of **1**, 1 atm of NH_3 was added and condensed, followed by 1 atm of SiH_4 (**Fig. 3a**). After 1 h at ambient temperature, precipitate began to form and the stepwise removal of H_2, unreacted SiH_4, and finally residual NH_3 after 24 h allowed for isolation of a light-yellow solid identified as PHPS (**Fig. 3b**). The FT-IR spectrum of this product (**Fig. 3c**) confirmed the presence of N–H (3358 cm^{-1}), Si–H (2118 cm^{-1}), Si–N (966 cm^{-1}) stretching vibrations, consistent with data that has previously been reported for PHPS.[45,46] As noted by Bauer and co-workers,[46] hydrolysis of this compound resulted in a significant decrease in Si–H and Si–N vibration absorbance over the course of 1 h at 13% humidity (**Table 3**). The CP-MAS ^{15}N NMR spectrum of our product was found to feature well-resolved resonances at 27.26 and 42.82 ppm in an approximate 1:1 ratio (**Fig. 3d**). The peak at 27.26 ppm is due to the presence of NSi_2H environments, while the resonance at 42.82 ppm can be attributed to tertiary NSi_3 moieties. Although the ^{15}N NMR shifts of silylamine compounds are sensitive to differences in silane substitution, our assignments are consistent with the trend reported for $(Me_3Si)_2NH$ (25.6 ppm) and $(Me_3Si)_3N$ (35.6 ppm).[47] Gratifyingly, the CP-MAS ^{29}Si NMR spectrum of our PHPS was found to exhibit a predominant resonance at -37.90 ppm along with a pair of spinning sidebands at 5 kHz spacing (**Fig. 3e**). Prior evaluations of PHPS by ^{29}Si NMR spectroscopy have assigned this peak to a mixture of SiN_2H_2 and SiN_3H environments,[16] which is consistent with our ^{15}N NMR data and the structure shown in **Fig. 3a**. The small resonance observed at -47.12 ppm has previously been assigned to quaternary silicon sites (SiN_4).[16,48] Overall, the multinuclear NMR spectra shown in **Fig. 3** suggest that the **1**-mediated dehydrocoupling of SiH_4 and NH_3 affords exceptionally pure PHPS. Adding SiH_4 to NH_3 in the absence of catalyst did not result in PHPS formation after 48 h at 25 °C.

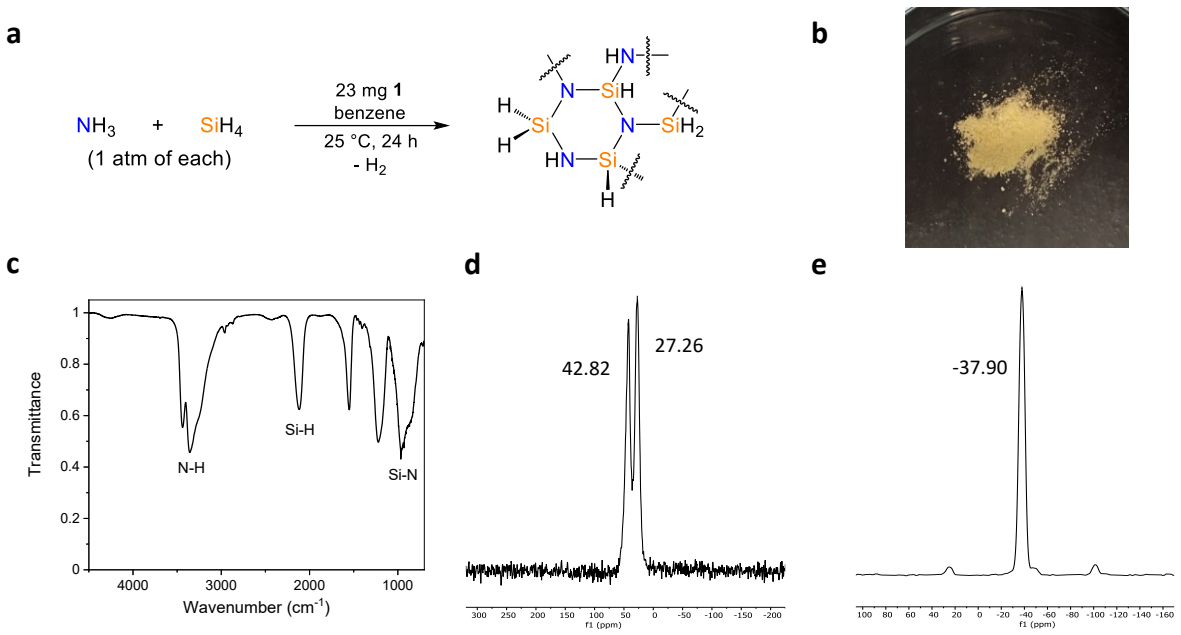

Fig. 3. Characterization of PHPS prepared using **1**. **a.** Synthetic conditions. **b.** Image of product. **c.** Solid-state infrared spectrum in KBr. **d.** ^{15}N CP-MAS NMR spectrum. **e.** ^{29}Si CP-MAS NMR spectrum.

Mechanistic Insight. Upon demonstrating that **1** generates Si–N bonds via dehydrocoupling, the mechanism of catalysis was explored. Initially, a J. Young tube containing a benzene-d_6 solution of **1** was subjected to 1 atm of SiH_4. Unmodified **1** was observed by ^{1}H NMR spectroscopy over the course of 24 h, indicating that this compound does not react with SiH_4 under the conditions of catalysis. Similarly, no reaction was observed when 2 equivalents of diisopropylamine (**1e**) were added to **1**. While preparing CVD precursors from the substrates in Table 1, we observed that the addition of unencumbered secondary amines to **1** resulted in instantaneous H_2 evolution. Adding 2 equivalents of methylethylamine (**1b**), diethylamine (**1c**), or dibutylamine (**1d**) to **1** revealed partial conversion to new paramagnetic species after 24 h by ^{1}H NMR spectroscopy (**1b**, 80%; **1c**, 50%; **1d**, 10%). Finally, when 2 equivalents of isopropylamine (**1f**) were added to **1**, complete conversion to the amido dimer [($^{2,6\text{-}i\text{Pr2Ph}}$BDI)Mn(μ-NH*i*Pr)]$_2$ (**2**, **Fig. 4a**) was observed after 24 h. This complex was found to exhibit paramagnetically broadened ^{1}H NMR resonances over a 35-ppm range and its magnetic susceptibility of 6.3 μ_B (25 °C) is consistent with the presence of high-spin Mn(II) and the value of 6.5 μ_B (25 °C) reported for imino(amido) dimer, [($^{2,6\text{-}i\text{Pr2Ph}}$BDI)Mn(μ-NCHPh)]$_2$.[38] The solid-state structure of **2** (**Fig. 4b**) revealed a pseudo-tetrahedral coordination environment about each metal center and a Mn–Mn distance of

3.0487(6) Å, indicative of a weak Mn-Mn bonding interaction.[39] One hydrogen atom on each bridging amido ligand was located in the difference map, confirming that these ligands are monoanionic and that the Mn centers of **2** are divalent.

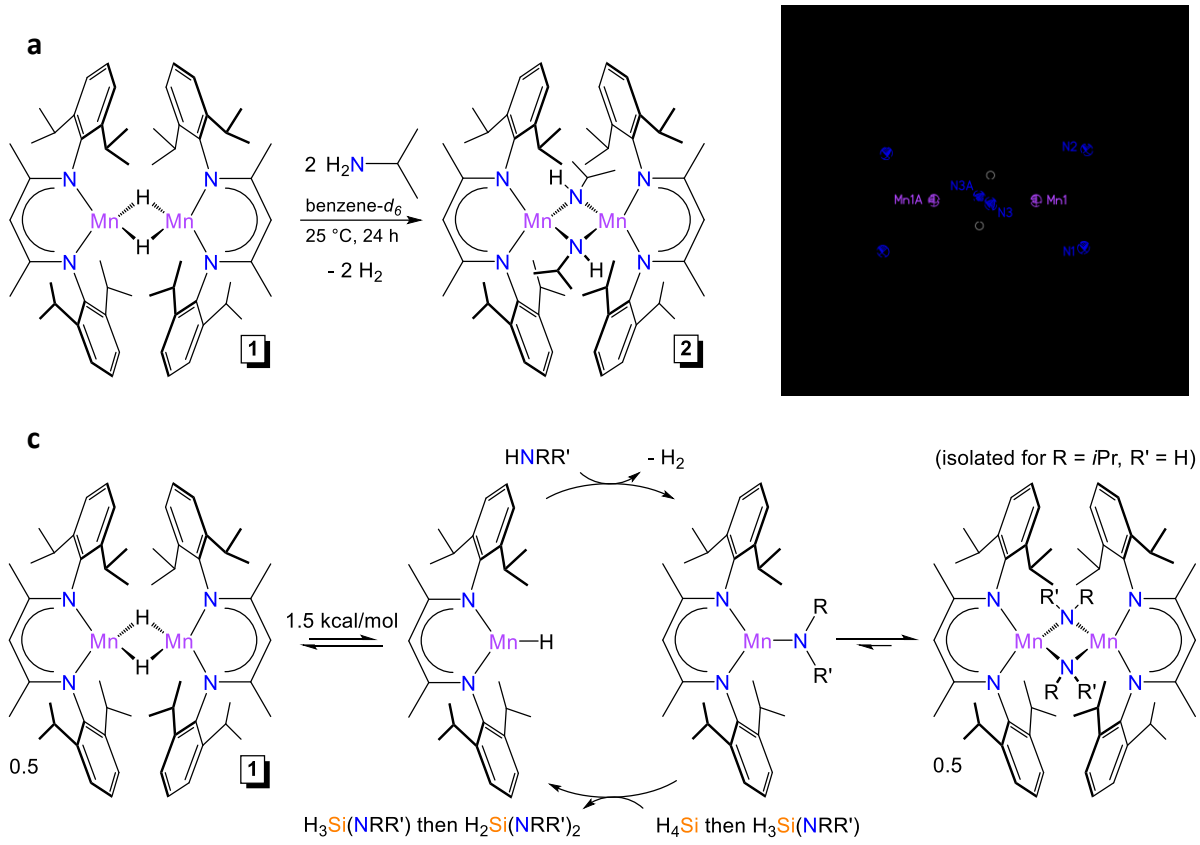

Fig. 4. Amine activation and the mechanism of dehydrocoupling. **a.** Addition of isopropylamine to **1** to yield **2. b.** Solid-state structure of **2. c.** Proposed mechanism of Si–N formation involving N-H and Si-H σ-bond metathesis.

In our recent communication of **1**-mediated nitrile hydroboration, we reported a barrier of 1.5 kcal/mol for the dissociation of **1** into two equivalents of ($^{2,6\text{-}i\text{Pr2Ph}}$BDI)MnH (**Fig. 4c**, left).[38] These monomers are readily available in solution at 25 °C, and when sterically unencumbered amines are present, Mn–H and N–H σ-bond metathesis occurs to eliminate H_2 and generate the corresponding amido intermediate (**Fig. 4c**, center). In the absence of SiH_4, these intermediates dimerize (**Fig. 4c**, right), which has allowed for the isolation of **2** in the case of isopropylamine. When an excess of SiH_4 was added to a benzene-d_6 solution of isolated **2**, complete conversion

to **1** was observed within 4 h at 25 °C. This result suggests that amido dimers including **2** are intermediates that can dissociate and undergo σ-bond metathesis with SiH_4 to regenerate **1** while forming the desired Si–N bond. A similar pathway was previously noted for **1**-mediated nitrile hydroboration.[38] Primary aminosilanes (i.e., H_3SiNRR') were not observed in this study and are believed to react preferentially with Mn amido intermediates to yield diaminosilane or triaminosilane products (**Fig. 4c**, bottom).

Additional experiments were performed to probe the sensitivity of Mn–N and Si–N bond formation to the presence of H_2, which represent the key steps of **1**-mediated dehydrocoupling (**Fig. 4c**, center). First, a benzene-*d*$_6$ solution of isolated **2** was subjected to 4 atm of H_2. No conversion to **1** and isopropylamine was observed over the course of 24 h at ambient temperature, suggesting that H_2 present in the headspace is unlikely to inhibit dehydrocoupling. Second, attempts to hydrogenate the Si–N bonds of $H_2Si(NEt_2)_2$ using 2 mol% of **1** under 4 atm of H_2 did not allow for the observation or SiH_4, diethylamine, or new aminosilanes over the course of 24 h at 25 °C. Therefore, once formed, it is believed that Si–N bonds are not reactivated by **1** under the conditions of catalysis.

DISCUSSION

The use of SiH_4 as a dehydrocoupling partner differentiates this study from prior efforts to catalyze Si–N bond formation. Although this reagent is not commonly found in academic settings, thousands of tons of SiH_4 are used each year to make polysilicon, rendering it an abundant and inexpensive synthetic precursor. It is also the only silicon source that can be used to prepare commercially-relevant CVD precursors via dehydrocoupling. Our exploration of **1**-mediated aminosilane synthesis suggests that the steric properties of the catalyst dictate both catalytic activity and product distribution. Although **1** enables the selective formation of secondary silanes such as $H_2Si(NEt_2)_2$ and $H_2Si(NH\textit{t}Bu)_2$, the diisopropylphenyl substituents of the chelate prevent **1** from generating tertiary or quaternary silanes when bulky secondary amines are used. Minimizing steric protection could allow for the design of catalysts that favor these products when they are desired.

To prepare PHPS via dehydrocoupling, SiH_4 is again the only silane source that can be used. The coupling of SiH_4 and NH_3 in the presence of **1** was found to result in highly cross-linked

PHPS powders that are insoluble in organic solvents. Solid PHPS can be used as a thermosetting resin or can be left to react with ammonia to yield solutions that leave behind silicon nitride or silicon oxynitride thin films. While films generated from PHPS are particularly useful for protecting electronic devices, organic polysilazanes are currently used to coat trains and automobiles. The polycarbosilazanes prepared from SiH_4 in this study represent sustainably-sourced alternatives to organic polysilazanes, which are currently prepared from chlorosilanes.

CONCLUSIONS

The manganese-catalyzed dehydrocoupling of amines to SiH_4 has allowed for the halogen-free synthesis of commercial aminosilane chemical vapor deposition precursors. These transformations were achieved using 1 atm of SiH_4 at ambient temperature. Extending the substrate scope to diamines and triamines allowed for the preparation of highly cross-linked polycarbosilanes, while the use of ammonia afforded solid perhydropolysilazane. When isopropylamine was independently added to $[(^{2,6\text{-}i\text{Pr2Ph}}\text{BDI})\text{Mn}(\mu\text{-H})]_2$, the corresponding amide dimer $[(^{2,6\text{-}i\text{Pr2Ph}}\text{BDI})\text{Mn}(\mu\text{-NH}i\text{Pr})]_2$ was isolated and characterized. This product was found to react with SiH_4 to regenerate the catalyst, indicating that Mn–N and H–Si σ-bond metathesis is responsible for Si–N formation. It is hoped that the atom-efficient aminosilane, polycarbosilazane, and perhydropolysilazane syntheses detailed in this contribution inspire the search for specialized catalysts and the industrial adoption of dehydrogenative Si–N bond formation.

EXPERIMENTAL DETAILS

General Considerations: All reactions were performed inside an MBraun glovebox under an atmosphere of purified nitrogen or on a high-vacuum manifold. Toluene, tetrahydrofuran, diethyl ether, and pentane were purchased from Sigma-Aldrich, purified using a Pure Process Technology solvent system, and stored in the glovebox over activated 4 Å molecular sieves and potassium in prior use. Benzene-d_6 was purchased from Oakwood Chemicals and dried over 4 Å molecular sieves and potassium prior to use. Toluene-d_8 and benzene were purchased from Sigma-Aldrich and dried over 4 Å molecular sieves and potassium prior to use. Tetramethylsilane was purchased from Sigma-Aldrich and dried over 4 Å molecular sieves. Celite was obtained from Oakwood Chemicals. Silane was obtained from Voltaix.

Dimethylamine, ethylmethylamine, dibutylamine, diisopropylamine, isopropylamine, *tert*-butylamine, ethylenediamine, diethylenetriamine, and tris(triaminoethyl)amine were purchased from Oakwood Chemicals. Diethylamine, bis(3-aminopropyl) terminated poly(dimethylsiloxane) ($M_n \approx 2{,}500$), poly(propylene glycol)-block-poly(ethylene glycol)-block-poly(propylene glycol) bis(2-aminopropyl ether), diaminopoly(ethylene glycol), and ammonia were purchased from Sigma Aldrich. All liquid substrates were dried over 4 Å molecular sieves prior to catalyst screening. $[(^{2,6\text{-iPr2Ph}}\text{BDI})\text{Mn}(\mu\text{-H})]_2$ (**1**) was synthesized according to literature procedure.[37]

Elemental analyses were performed at Midwest Microlab (Indianapolis, IN). Infrared spectra were collected on a Bruker VERTEX 70 spectrophotometer with an MCT detector. Solution nuclear magnetic resonance (NMR) spectra were recorded at room temperature on a Varian 400 MHz or a Bruker 400 MHz NMR spectrometer. All ^{1}H NMR and ^{13}C NMR chemical shifts (ppm) are reported relative to $Si(Me)_4$ using ^{1}H (residual) and ^{13}C chemical shifts of the solvent as secondary standards. ^{29}Si NMR chemical shifts (ppm) are reported relative to $Si(Me)_4$ using the absolute ^{1}H NMR frequency of an internal $Si(Me)_4$ standard. Solid state NMR spectra were recorded at room temperature on a wide-bore 400 MHz solid-state AVANCE NMR instrument (Bruker). Air-sensitive samples were packed into 4 mm zirconia magic-angle spinning (MAS) rotors in an inert atmosphere glovebox and spun at 5 kHz. CP-MAS experiments were performed such that the measurements could rely on the increased sensitivity and shorter relaxation time provided by the protons. A relaxation delay of approximately 3 s was used between acquisitions and measurement time ranged from 12 to 24 hr, depending on the concentration of ^{29}Si and ^{15}N in each material. For ^{15}N CP-MAS measurements, the ^{1}H $\pi/2$ pulse was 4.1 μsecs, 1.5 msec contact time and SPINAL64 decoupling. All ^{15}N CP-MAS NMR chemical shifts (ppm) are reported relative to a saturated NH_4^+ solution at 0 ppm (unified scale) using α-glycine (33.4 ppm) as an external standard. For ^{29}Si CP-MAS experiments the ^{1}H $\pi/2$ pulse was 6.0 μsecs, 3.0 msec contact time and SPINAL64 decoupling. All ^{29}Si NMR chemical shifts are referenced relative to $Si(Me)_4$ using tetrakis(trimethylsilyl)silane (-8.9 ppm) as an external standard.

X-ray Crystallography: Low-temperature X-ray diffraction data for **2** were collected on a Rigaku XtaLAB Synergy diffractometer coupled to a Rigaku Hypix detector with Cu Kα radiation (λ = 1.54184 Å), from a PhotonJet micro-focus X-ray source at 100 K. The diffraction images were processed and scaled using the CrysAlisPro software. The structures were solved

through intrinsic phasing using SHELXT and refined against F^2 on all data by full-matrix least squares with SHELXL following established refinement strategies. These data were refined as a 2-component twin with a BASF factor of 0.2144(7). All non-hydrogen atoms were refined anisotropically. All hydrogen atoms bound to carbon were included in the model at geometrically calculated positions and refined using a riding model. Hydrogen atoms bound to nitrogen were located in the difference Fourier synthesis and subsequently refined semi-freely with the help of distance restraints. The isotropic displacement parameters of all hydrogen atoms were fixed to 1.2 times the Ueq value of the atoms they are linked to (1.5 times for methyl groups). Details of the data quality and a summary of the residual values of the refinements are listed in Tables S1-S6.

MALDI-TOF Mass Spectrometry: Samples were analyzed on a Bruker microFlex LRF instrument (Billerica, MA, USA) with a 337 nm laser in positive mode scanning from 200 to 200,000 *m/z*. The ion source 1 voltage was 19.50 kV, ion source 2 voltage was 18.15 kV, the lens voltage was 7.00 kV, and ion suppression was off.

General Procedure for Preparing CVD Compounds using a Liquid Amine: Under N_2 atmosphere, a J. Young tube was charged with 0.010 g (0.010 mmol) of **1** in 0.4 mL of 0.2 M TMS in toluene-d_8, followed by 0.50 mmol of amine. The tube was sealed under N_2 and attached to the vacuum line. The solution was frozen in liquid N_2, gas was removed from the head space under vacuum, and 1 atm of SiH_4 was introduced. ***DANGER: SiH_4 will react violently with air and must be added under vacuum.*** The tube was closed, disconnected from the vacuum line, and placed in a steel container to warm to room temperature in the back of an empty fume hood with the sash closed. The reaction was allowed to occur at ambient temperature for 24 h. Multinuclear NMR data was collected after 24 h, conversion was determined by examining the consumption of starting amine ^{1}H NMR resonances, and NMR yields were determined by integrating the products against the internal TMS standard. To safely end the experiment, the tube was attached to the vacuum line, the solution was frozen in liquid N_2, and H_2 was removed under vacuum. Residual SiH_4 was recollected in a lecture bottle (preferred) or allowed to slowly evaporate through repeated warming and cooling of the solution in liquid N_2 under dynamic vacuum. Allowing H_2 and SiH_4 mixtures to disperse in a large volume of N_2 that can be purged

in a controlled manner (i.e., by opening the tube in a glovebox) proved to be a safe alternative to slow removal under vacuum. ***See the Supporting Information for additional safety disclosures.***

General Procedure for Preparing Polycarbosilazanes: Under N_2 atmosphere, a 100 mL thick-walled glass bomb was charged with 0.020 g (0.021 mmol) of **1** in 3 mL benzene, followed by 1.05 mmol of amine. The evolution of hydrogen gas was observed instantly. The bomb was sealed under N_2 and attached to the vacuum line. The solution was frozen in liquid N_2, gas was removed from the head space under vacuum, and 1 atm of SiH_4 was introduced. ***DANGER: SiH_4 will react violently with air and must be added under vacuum.*** The bomb was closed, disconnected from the vacuum line, and placed in a steel container to warm to room temperature in the back of an empty fume hood with the sash closed. Polycarbosilazane precipitate was observed after 2 h and the reactions were allowed to occur at ambient temperature for 24 h. The bomb was then attached to the vacuum line, the solution was frozen in liquid N_2, and H_2 was removed under vacuum. Following H_2 removal, residual SiH_4 was recollected in a lecture bottle (preferred) or allowed to slowly evaporate through repeated warming and cooling of the solution in liquid N_2 under dynamic vacuum. ***See the Supporting Information for additional safety disclosures.*** The bomb was brought into the glove box, the product was washed with THF (2 x 5 mL) and pentane (2 x 5 mL) then dried *in vacuo* to isolate the corresponding polycarbosilazane.

ASSOCIATED CONTENT

Supporting Information. The Supporting Information is available free of charge on the ACS Publications website. An extensive description of experimental procedures, spectroscopic characterization, and crystallographic information. (PDF)

Accession Codes. CCDC 2089709 contains the supplementary crystallographic data for this paper. These data can be obtained free of charge via www.ccdc.cam.ac.uk/data_request/cif, or by emailing data_request@ccdc.cam.ac.uk or by contacting the Cambridge Crystallographic Data Centre, 12 Union Road, Cambridge CB2 1EZ, UK; fax: +44 1223 336033.

AUTHOR INFORMATION

Corresponding Author

**ryan.trovitch@asu.edu*

ORCID

Thao T. Nguyen: 0000-0002-5545-7441

Samantha N. MacMillan: 0000-0001-6516-1823

Michael T. Janicke: 0000-0002-3139-2882

Ryan J. Trovitch: 0000-0003-4935-6780

Notes

T.T.N., T.K.M., and R.J.T. retain rights to compounds **1** and **2** through U.S. Patent Application Nos. 62/678,624 (2018) and 16/407,317 (2019).

ACKNOWLEDGMENTS

This material is based upon work supported by the National Science Foundation under Grant No. 1651686. We would like to acknowledge Dr. Megan M. Maurer for assistance with mass spectrometry.

REFERENCES

1. Philipp, H. R. Optical Properties of Silicon Nitride. *J. Electrochem. Soc.* **1973**, *120*, 295–299.

2. de Brito Mota, F.; Justo, J. F.; Fazzio, A. Structural Properties of Amorphous Silicon Nitride. *Phys. Rev. B* **1998**, *58*, 8323–8328.

3. Kaloyeros, A. E.; Pan, Y.; Goff, J.; Arkles, B. Review—Silicon Nitride and Silicon Nitride-Rich Thin Film Technologies: State-of-the-Art Processing Technologies, Properties, and Applications. *ECS J. Solid State Sci. Technol.* **2020**, *9*, 063006.

4. Khomenkova, L.; Normand, P.; Gourbilleau, F.; Slaoui, A.; Bonafos, C. Optical, Structural and Electrical Characterizations of Stacked Hf-Based and Silicon Nitride Dielectrics. *Thin Solid Films* **2016**, *617*, 143–149.

5. Kaga, Y.; Kikuchi, H.; Imamura, H.; Watanabe, J. Silicon Nitride Substrate, A Manufacturing Method of the Silicon Nitride Substrate, A Silicon Nitride Wiring Board using the Silicon Nitride Substrate, and Semiconductor Module. U.S. Patent No. 7,915,533 (2011).

6. Kuo, Y. Plasma Enhanced Chemical Vapor Deposited Silicon Nitride as a Gate Dielectric Film for Amorphous Silicon Thin Film Transistors—a Critical Review. *Vacuum* **1998**, 51, 741–745.

7. El amrani, A.; Menous, I.; Mahiou, L.; Tadjine, R.; Touati, A.; Lefgoum, A. Silicon Nitride Film for Solar Cells. *Renewable Energy* **2008,** *33*, 2289–2293.
8. van Assche, F. J. H.; Unnikrishnan, S.; Michels, J. J.; van Mol, A. M. B.; van de Weijer, P.; van de Sanden, M. C. M.; Creatore, M. On the Intrinsic Moisture Permeation Rate of Remote Microwave Plasma-Deposited Silicon Nitride Layers. *Thin Solid Films* **2014**, *558*, 54–61.
9. Roenigk K. F.; Jensen K. F. Low-Pressure CVD of Silicon Nitride. *J. Electrochem. Soc.* **1987**, *134*, 1777–1785.
10. Niskanen, A. J.; Chen, S.; Pore, V.; Fukazawa, A.; Fukuda, H.; Haukka, S. P. Si Precursors for Deposition of SiN at Low Temperatures. U.S. Patent No. 9,564,309 (2017).
11. Yusup, L. L.; Park, J.-M.; Noh, Y.-H.; Kim, S.-J.; Lee, W.-J.; Park, S.; Kwon, Y.-K. Reactivity of Different Surface Sites with Silicon Chlorides during Atomic Layer Deposition of Silicon Nitride. *RSC Adv.* **2016**, 6, 68515–68524.
12. Laxman, R. K.; Roberts, D. A.; Hochberg, A. K.; Hockenhull, H. G.; Kaminsky, F. D. Silicon Nitride from Bis(Tertiarybutylamino)Silane. U.S. Patent No. 5,874,368 (1999).
13. Kim, K.-H. Fabrication and Properties of Silicon-Nitride Films Deposited by Using PECVD with a Tris(Dimethylamino)Silane of Aminosilane Precursor. *J. Korean Phys. Soc.* **2015**, *67*, 2115–2119.
14. Aylett, B. J.; Emsley, J. The Preparation and Properties of Dimethylamino- and Diethylaminosilane. *J. Chem. Soc. A* **1967**, 652–655.
15. Anderson, D. G.; Rankin, D. W. H. Isopropyldisilylamine and Disilyl-t-Butylamine: Preparation, Spectroscopic Properties, and Molecular Structure in the Gas Phase, Determined by Electron Diffraction. *J. Chem. Soc., Dalton Trans.* **1989**, 779–783.
16. Schwab, S. T.; Graef, R. C.; Blanchard, C. R.; Dec, S. F.; Maciel, G. G. The Pyrolytic Conversion of Perhydropolysilazane into Silicon Nitride. *Ceram. Int.* **1998**, *24*, 411–414.
17. Wang, K.; Zheng, X.; Ohuchi, F. S.; Bordia, R. K. The Conversion of Perhydropolysilazane into SiON Films Characterized by X-Ray Photoelectron Spectroscopy. *J. Am. Ceram. Soc.* **2012**, **95**, 3722–3725.
18. Zhang, Z.; Shao, Z.; Luo, Y.; An, P.; Zhang, M.; Xu, C. Hydrophobic, Transparent and Hard Silicon Oxynitride Coating from Perhydropolysilazane. *Polym. Int.* **2015**, *64*, 971–978.

19. Kang, Y. H.; Min, B. K.; Kim, S. K.; Bae, G.; Song, W.; Lee, C.; Cho, S. Y.; An, K.-S. Proton Conducting Perhydropolysilazane-Derived Gate Dielectric for Solution-Processed Metal Oxide-Based Thin-Film Transistors. *ACS Appl. Mater. Interfaces* **2020**, *12*, 15396–15405.
20. Seyferth, D.; Wiseman, G. H.; Prud'homme, C. A Liquid Silazane Precursor To Silicon Nitride. *J. Am. Ceram. Soc.* **1983**, *66*, C13–C14.
21. Schwab, S. T. Polysilazane Precursors for Silicon Nitride and Resultant Products. U.S. Patent No. 5,294,425 (1994).
22. Liu, H. Q.; Harrod, J. F. Dehydrocoupling of Ammonia and Silanes Catalyzed by Dimethyltitanocene. *Organometallics* **1992**, *11*, 822-827.
23. Reuter, M. B.; Hageman, K.; Waterman, R. Silicon-Nitrogen Bond Formation via Heterodehydrocoupling and Catalytic N-Silylation. *Chem. Eur. J.* **2021**, 27, 3251-3261.
24. Dunne, J. F.; Neal, S. R.; Engelkemier, J.; Ellern, A.; Sadow, A. D. Tris(Oxazolinyl)Boratomagnesium-Catalyzed Cross-Dehydrocoupling of Organosilanes with Amines, Hydrazine, and Ammonia. *J. Am. Chem. Soc.* **2011**, *133*, 16782–16785.
25. Hill, M. S.; Liptrot, D. J.; MacDougall, D. J.; Mahon, M. F.; Robinson, T. P. Hetero-Dehydrocoupling of Silanes and Amines by Heavier Alkaline Earth Catalysis. *Chem. Sci.* **2013**, **4**, 4212–4222.
26. Bellini, C.; Dorcet, V.; Carpentier, J.-F.; Tobisch, S.; Sarazin, Y. Alkaline-Earth-Catalysed Cross-Dehydrocoupling of Amines and Hydrosilanes: Reactivity Trends, Scope and Mechanism. *Chem. Eur. J.* **2016**, *22*, 4564–4583.
27. Li, N.; Guan, B.-T. A Dialkyl Calcium Carbene Adduct: Synthesis, Structure, and Catalytic Cross-Dehydrocoupling of Silanes with Amines. *Eur. J. Inorg. Chem.* **2019**, 2231–2235.
28. Pindwal, A.; Ellern, A.; Sadow, A. D. Homoleptic Divalent Dialkyl Lanthanide-Catalyzed Cross-Dehydrocoupling of Silanes and Amines. *Organometallics* **2016**, *35*, 1674–1683.
29. Yonekura, K.; Iketani, Y.; Sekine, M.; Tani, T.; Matsui, F.; Kamakura, D.; Tsuchimoto, T. Zinc-Catalyzed Dehydrogenative Silylation of Indoles. *Organometallics* **2017**, *36*, 3234–3249.
30. Ríos, P.; Roselló-Merino, M.; Rivada-Wheelaghan, O.; Borge, J.; López-Serrano, J.; Conejero, S. Selective Catalytic Synthesis of Amino-Silanes at Part-per Million Catalyst Loadings. *Chem. Commun.* **2018**, *54*, 619–622.
31. Allen, L. K.; García-Rodríguez, R. & Wright, D. S. Stoichiometric and Catalytic Si–N Bond Formation Using the p-Block Base $Al(NMe_2)_3$. *Dalton Trans.* **2015**, *44*, 12112–12118.

32. Bellini, C.; Orione, C.; Carpentier, J.-F.; Sarazin, Y. Tailored Cyclic and Linear Polycarbosilazanes by Barium-Catalyzed N–H/H–Si Dehydrocoupling Reactions. *Angew. Chem. Int. Ed.* **2016**, *55*, 3744-3748.
33. Bellini, C.; Roisnel, T.; Carpentier, J.-F.; Tobisch, S.; Sarazin, Y. Sequential Barium-Catalysed N−H/H−Si Dehydrogenative Cross-Couplings: Cyclodisilazanes versus Linear Oligosilazanes. *Chem. Eur. J.* **2016**, *22*, 15733–15743.
34. Morris, L. J.; Whittell, G. R.; Eloi, J.-C.; Mahon, M. F.; Marken, F.; Manners, I.; Hill, M. S. Ferrocene-Containing Polycarbosilazanes via the Alkaline-Earth-Catalyzed Dehydrocoupling of Silanes and Amines. *Organometallics* **2019**, *38*, 3629–3648.
35. Gasperini, D.; King, A. K.; Coles, N. T.; Mahon, M. F.; Webster, R. L. Seeking Heteroatom-Rich Compounds: Synthetic and Mechanistic Studies into Iron Catalyzed Dehydrocoupling of Silanes. *ACS Catal.* **2020**, *10*, 6102–6112.
36. Barroso, G.; Döring, M.; Horcher, A.; Kienzle, A.; Motz, G. Polysilazane-Based Coatings with Anti-Adherent Properties for Easy Release of Plastics and Composites from Metal Molds. *Adv. Mater. Interfaces* **2020**, *7*, 1901952.
37. Mukhopadhyay, T. K.; Flores, M.; Groy, T. L.; Trovitch, R. J. A β-Diketiminate Manganese Catalyst for Alkene Hydrosilylation: Substrate Scope, Silicone Preparation, and Mechanistic Insight. *Chem. Sci.* **2018**, *9*, 7673–7680.
38. Nguyen, T. T.; Kim, J.-H.; Kim, S.; Oh, C.; Flores, M.; Groy, T. L.; Baik, M.-H.; Trovitch, R. J. Scope and Mechanism of Nitrile Hydroboration Mediated by a β-Diketiminate Manganese Hydride Catalyst. *Chem. Commun.* **2020**, *56*, 3959–3962.
39. Oh, C.; Siewe, J.; Nguyen, T. T.; Kawamura, A.; Flores, M.; Groy, T. L.; Anderson, J. S.; Trovitch, R. J.; Baik, M.-H. "The Electronic Structure of a β-Diketiminate Manganese Hydride Dimer." *Dalton Trans.* **2020**, *49*, 14463-14474.
40. Sanchez, A.; Itov, G.; Zhang, P.; Stephens, M. D.; Khandelwal, M. Halogen Free Syntheses of Aminosilanes by Catalytic Dehydrogenative Coupling. U.S. Patent Application No. 2018/0230171 (2018).
41. Levy, R. A.; Lin, X.; Grow, J. M.; Boeglin, H. J.; Shalvoy, R. Low Pressure Chemical Vapor Deposition of Silicon Nitride Using the Environmentally Friendly Tris(Dimethylamino)Silane Precursor. *J. Mater. Res.* **1996**, *11*, 1483–1488.

42. Gumpher, J.; Bather, W.; Mehta, N.; Wedel, D. Characterization of Low-Temperature Silicon Nitride LPCVD from Bis(tertiary-butylamino)silane and Ammonia. *J. Electrochem. Soc.* **2004**, *151*, G353-G359.
43. Smith, A. L. Infrared Spectra-Structure Correlations for Organosilicon Compounds. *Spectrochimica Acta* **1960**, *16*, 87–105.
44. Abel, A. E.; Kruger, T. A.; Mouk, R. W.; Knasiak, G. J. Silazane and/or Polysilazane Compounds and Methods of Making. U.S. Patent No. 6,329,487 (2001).
45. Iwamoto, Y.; Kikuta, K.; Hirano, S. Si_3N_4–TiN–Y_2O_3 Ceramics Derived from Chemically Modified Perhydropolysilazane. *J. Mater. Res.* **1999**, *14*, 4294–4301.
46. Bauer, F.; Decker, U.; Dierdorf, A.; Ernst, H.; Heller, R.; Liebe, H.; Mehnert, R. Preparation of Moisture Curable Polysilazane Coatings: Part I. Elucidation of Low Temperature Curing Kinetics by FT-IR Spectroscopy. *Prog. Org. Coat.* **2005**, *53*, 183–190.
47. Witanowski, M.; Stefaniak, I.; Webb, G. A. Nitrogen NMR Spectroscopy. In *Annual Reports on NMR Spectroscopy*; Webb, G. A., Ed.; Academic Press, 1978; Vol. 7, pp 117–244.
48. Lewis, R. H.; Maciel, G. E. Magnetic Resonance Characterization of Solid-state Intermediates in the Generation of Ceramics by Pyrolysis of Hydridopolysilazane. *J. Mater. Sci.* 1995, **30**, 5020-5030.

For Table of Contents Use Only:

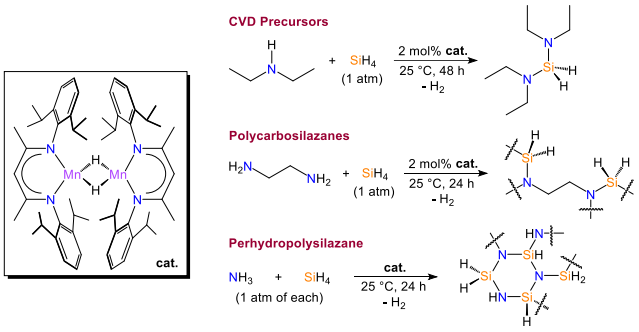

Manganese-catalyzed dehydrogenative coupling has allowed for the halogen-free and atom-efficient preparation of aminosilane monomers, polycarbosilazanes, and perhydropolysilazane.